Gargouri et al. Journal of Theoretical and Applied Physics 2013, 7:29
http://www.jtaphys.com/content/7/1/29

Journal of Theoretical and Applied Physics
a SpringerOpen Journal

RESEARCH Open Access

Packet charge dynamic in thin polyethylene under high dc voltage

Amal Gargouri, Imed Boukhris*, Ezzeddine Belgaroui and Ali Kallel

Abstract

In this paper, we present a bipolar transport model in low-density polyethylene under high direct-current voltage in order to investigate the charge packet dynamic generated under high injection. These charge packets, observed by our model for the first time, have already been seen in some previous experimental works for a long time. Our model results show that applied electric field and sample thickness play important roles on the apparition of space charge packets.

Keywords: LDPE, High dc voltage, Charge packet

Introduction

Low-density polyethylene (LDPE) is considered as the material mostly used in high-voltage insulation, thanks to its important mechanical and electrical properties [1]. Unfortunately, several previous experimental works that were realized on charge transport in polyethylene proved that space charge accumulation phenomenon affects the electrical properties of the insulator and can lead to its electrical breakdown [2-4]. In 1994, Alison started the first attempt on bipolar charge transport model, and he evoked consistent theoretical formulations for this problem [5]. After that, several modeling works interesting to bipolar charge transport appeared based on Alison's model [6-9]. In this work, we present a bipolar charge transport model for low and high direct-current (dc) voltage, taking into account trapping, detrapping, and recombination phenomena [10]. The theoretical formulation of the problem regroups three coupled equations: Poisson's equation, continuity equation, and transport equation. To resolve this bipolar problem, we apply adequate numerical techniques. Indeed, the sample thickness is divided into cells of trapping, detrapping, and recombination phenomena. In the first step, we apply the finite element method to Poisson's equation in order to determine the instantaneous electric field distribution of the inputs and outputs of cells. In the second step, we apply the Leonard model to the continuity equation without source terms to determine the mobile charge densities (electrons and holes) in each cell. Finally, these mobile charge densities are used as initial data for the Runge-Kutta method, of the precision degree 5, applied to the continuity equation with source terms for the purpose of determining the densities of mobile and trapped electrons and holes. Details of the model were presented in our previous works [10,11]. By this, we proved the existence of two charge dynamics under low and high dc voltages, respectively. In fact, under low applied dc voltage, the charge dynamic in the polyethylene sample is dominated by trapped charges, and the results of external current show the aspect of space charge-limited current, whereas under high dc voltage, the charge packet aspect appears, and the charge dynamic and the evolution of the external current density are governed by mobile charges [11]. These aspects were also shown experimentally in previous works [12]. In this work, we focused on the conditions of charge packet apparition. In fact, there is a threshold value of the voltage from which the charge packet aspect appears and the charge dynamic changes. To explain this effect, two parameters are considered: the sample thickness and the value of applied electric field. Our model results show a threshold value to observe charge packet aspect for both parameters, and the dynamic is always governed by mobile charges.

Physical model

Our work is realized on an isotherm low-density polyethylene of 150-μm thickness sandwiched between two electrodes under dc applied voltage. The holes and

* Correspondence: Email: imed_boukhris@yahoo.fr
Laboratoire des Matériaux Composites Céramiques et Polymères (LaMaCoP)
Faculté des sciences de Sfax, BP 805, Sfax 3000, Tunisia

electrons were injected according to the Schottky model and had an effective mobility which was exponentially dependent on the temperature. As the sample is an isotherm, then the effective mobility is constant. Two kinds of traps exist in the bulk of the sample: shallow traps (due to chain polymer conformation) which contribute to the conduction phenomenon (transport) and deep traps (due to chemical impurities) which contribute to the trapping mechanism and charge accumulation which can lead to many problems and even to the electrical breakdown of the insulator [13,14].

Theoretical formulation

Our model is based on three coupled equations: Poisson's equation, continuity equation, and transport equation.

Poisson's equation is written as follows:

$$\frac{\partial^2 V(x,t)}{\partial x^2}+\frac{\rho(x,t)}{\varepsilon}=0;0<x<D, \tag{1}$$

$$\overrightarrow{\text{grad}}\ (V(x,t))=-\vec{E}\ (x,t). \tag{2}$$

Continuity equation is written as follows:

$$\frac{\partial \rho_{(e,h)\mu}(x,t)}{\partial t}+\frac{\partial j_{(e,h)}(x,t)}{\partial x}=S_{t(e,h)}(x,t)+S_{r(e,h)}(x,t)+S_{\mathrm{dt}(e,h)}(x,t). \tag{3}$$

$S_{t(e,h)}$, $S_{\mathrm{dt}(e,h)}$, and $S_{r(e,h)}$ are the source terms of trapping, detrapping, and recombination mechanisms, respectively:

$$S_{t(e(\mathrm{or})h)}(x,t)=\pm B_{(e(\mathrm{or})h)}\rho_{\mathrm{et(or)ht}}(x,t)\times\left(1-\frac{\rho_{\mathrm{et(or)ht}}{}^{(x,t)}}{d\rho_{(\mathrm{et(or)ht})}}\right), \tag{4}$$

$$S_{dt(e(or)h)}(x,t)=\pm D_{dt(\mathbf{e}(or)\mathbf{h})}\rho_{et(or)ht}(x,t), \tag{5}$$

with

$$D_{\mathrm{dt}(e(\mathrm{or})h)}=\nu\exp\left(\frac{-e\mathrm{w}_{d(e(\mathrm{or})h)}}{kT}\right), \tag{6}$$

$$S_r(x,t)=S_{r(\mathrm{e\mu,ht})}(x,t)+S_{r(\mathrm{et,h\mu})}(x,t)+S_{r(\mathrm{et,ht})}(x,t), \tag{7}$$

where $d\rho_{(\mathrm{et(or)ht})}$ are the trapped densities for electrons and holes. For the coefficient of trapping (B), signs (+) and (−) correspond respectively to the appearance of trapped charges and the disappearance of mobile charges. For the coefficient of detrapping (D_{dt}), signs (+) and (−) correspond to the appearance of mobile charges and the disappearance of trapped charges, respectively. w_{de} and w_{dh} are the detrapping barriers for electrons and holes, respectively. ν is the attempt to escape the frequency.

Finally, transport equation is written as follows:

$$j_{(e,h)}(x,t)=\mu_{e,h}\rho_{(e,h)\mu}(x,t)E(x,t). \tag{8}$$

The following equation describes the condition of an additive-free sample:

$$\rho(x,0)\approx 0. \tag{9}$$

The boundary conditions related to the applied voltages at the cathode and the anode are given by the following equations, respectively:

$$V(0,t>0)=V_C, \tag{10}$$

$$V(D,t>0)=V_A, \tag{11}$$

with

$$\int_0^D Edx=\Delta V, \tag{12}$$

$$\Delta V=V_C-V_A. \tag{13}$$

Flows of injected electrons and holes are given by the Schottky model as follows, respectively:

$$j_e(0,t)=AT^2\exp\left(-\frac{w_{ei}}{kT}\right)\exp\left(\frac{e}{kT}\sqrt{\frac{eE(0,t)}{4\pi\varepsilon}}\right), \tag{14}$$

$$j_h(D,t)=AT^2\exp\left(-\frac{w_{hi}}{kT}\right)\exp\left(\frac{e}{kT}\sqrt{\frac{eE(D,t)}{4\pi\varepsilon}}\right). \tag{15}$$

Table 1 Nomenclature

Parameters	Fixed values
Coefficients of trapping	
B_{e} (electrons)	7×10^{-3} s^{-1}
B_{h} (holes)	7×10^{-3} s^{-1}
Coefficients of recombination	
S_0	4×10^{-3} m^3 C^{-1} s^{-1}
S_1	4×10^{-3} m^3 C^{-1} s^{-1}
S_2	4×10^{-3} m^3 C^{-1} s^{-1}
S_3	Neglected (0)
Mobilities	
μ_e (electron)	9×10^{-15} m^2 V^{-1} s^{-1}
μ_h (hole)	9×10^{-15} m^2 V^{-1} s^{-1}
Trap density	
dpe (electrons)	100 C m^{-3}
dpt (holes)	100 C m^{-3}
Injection barriers	
w_{ei} (electrons)	1.2 eV
w_{hi} (holes)	1.2 eV
Temperature	25°C
Applied voltage	10 and 50 kV
Time step	0.01 s
Sample thickness	150 μm
Spatial discretization	Variable

Equations of conduction, displacement, and external currents

The conduction current density for the mobile electrons and holes is written in the following way:

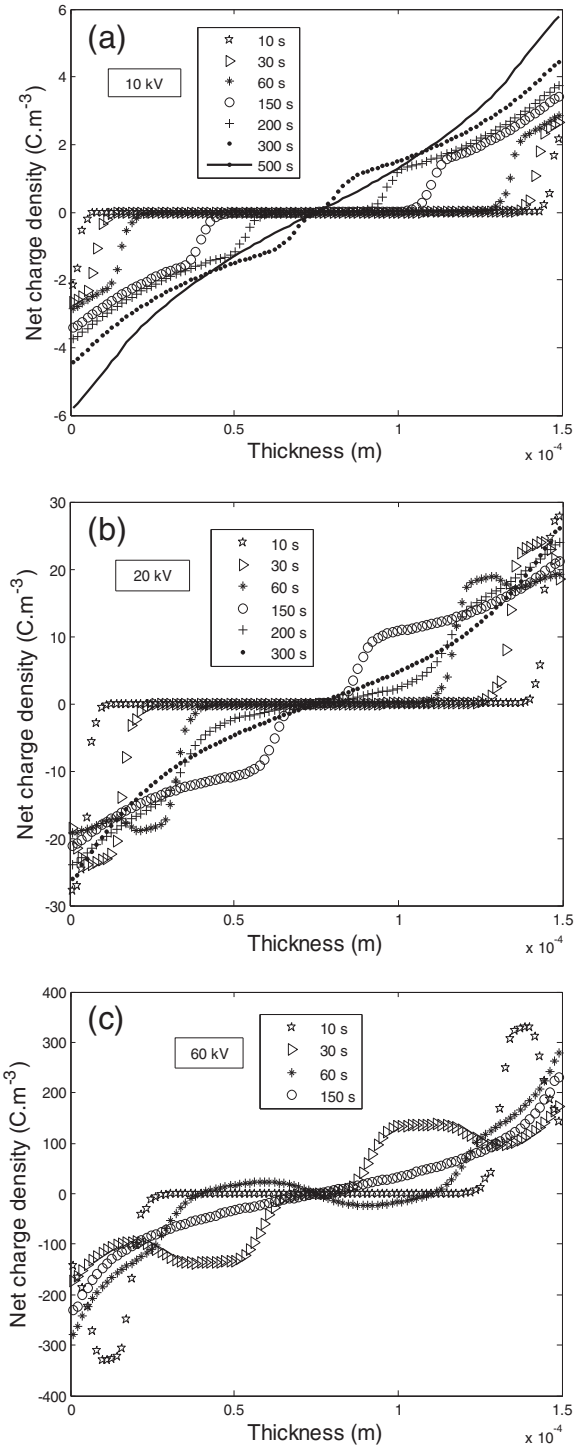

Figure 1 Net charge density in a thickness of 150×10^{-6} m. Under (**a**) 10, (**b**) 20, and (**c**) 60 kV.

$$j_{e\mu,h\mu}(x,t) = \left(\mu_e \rho_{e\mu}(x,t) + \mu_h \rho_{h\mu}(x,t)\right) E(x,t). \quad (16)$$

The displacement current density is as follows:

$$j_d(x,t) = \varepsilon \frac{\partial E(x,t)}{\partial t}. \quad (17)$$

The external current density is given by the following equation:

$$J(t) = j_{e\mu,h\mu}(x,t) + j_d(x,t). \quad (18)$$

Due to the boundary condition (Equation 12), the following condition is always satisfied:

$$\int_0^D j_d(x,t)dx = 0 \quad (19)$$

Nomenclature of different model coefficients and parameters is given in Table 1.

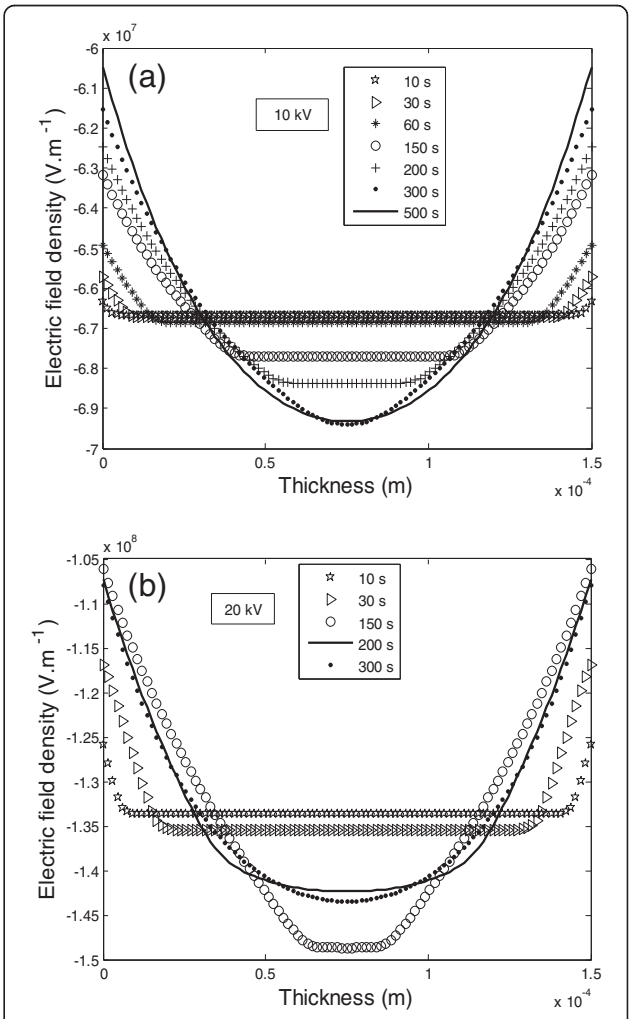

Figure 2 Electric field distributions in a thickness of 150×10^{-6} m. (**a**) 10 and (**b**) 20 kV.

Results and discussion

In this section, we study the effects of the applied electric field and the sample thickness on the apparition of the space charge packets and on the dynamic of charge.

Effect of applied electric field

Figure 1a,b,c shows the net charge density in the bulk of an LDPE sample of 150-μm thickness under 10, 20, and 60 kV, respectively. From Figure 1a, we note the absence of charge packets and the accumulation of injected electrons and holes near the electrodes. Figure 1b gives the first apparition of the charge packets which are more significant in Figure 1c. Under 60 kV of dc voltage, we note also the presence of alternation zones called zones of heterocharges (profile at 60 s). From these results, we can conclude that the charge packets are linked to the threshold value of applied voltage of about 20 kV, which corresponds to an applied electric field of 1.33×10^8 V m^{-1}.

Figure 2a,b shows the electric field distribution under 10 and 20 kV, respectively. From this figure, we can conclude that the apparition of space charge packets under a high voltage is due to the reintensification of electric field at the interfaces which provokes the intensification of injected charge densities. In fact, as can be seen from Figure 2a, there is no intensification of the interfacial electric field which decreases continuously because of the accumulation of injected charges near the electrodes. This can explain the disappearance of charge packets under low dc voltage. However, in Figure 2b, the reintensification of the electric field at the interfaces is clearly observed as it can be seen from profile 200 s.

To understand how the charges behave at low and high voltages, we plot the mobile and the trapped electron densities under 10 and 60 kV. Figure 3a,b shows the electron densities at 10 kV. From this figure, it is clearly observed that the trapped electron density is much higher than the

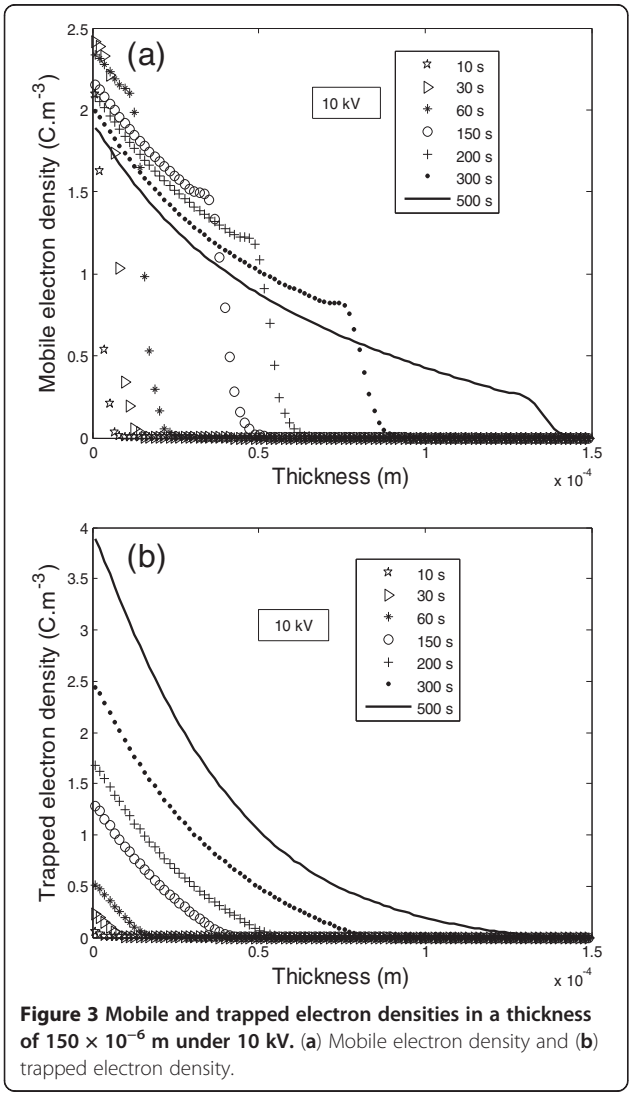

Figure 3 Mobile and trapped electron densities in a thickness of 150 × 10^{-6} m under 10 kV. (**a**) Mobile electron density and (**b**) trapped electron density.

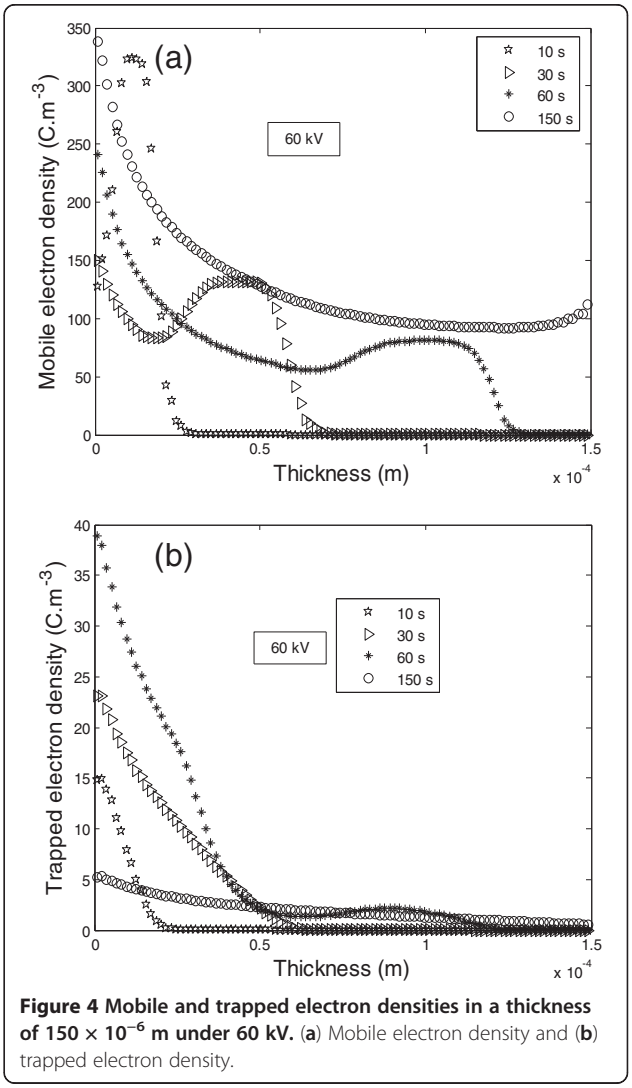

Figure 4 Mobile and trapped electron densities in a thickness of 150 × 10^{-6} m under 60 kV. (**a**) Mobile electron density and (**b**) trapped electron density.

mobile density. In fact, the trapped electron density is almost equal to 4 C m^{-3} and the mobile electron density is nearly equal to 2 C m^{-3}. Thus, we can conclude that under a low voltage (less than 20 kV dc applied voltage), the charge dynamic is governed by trapped charges.

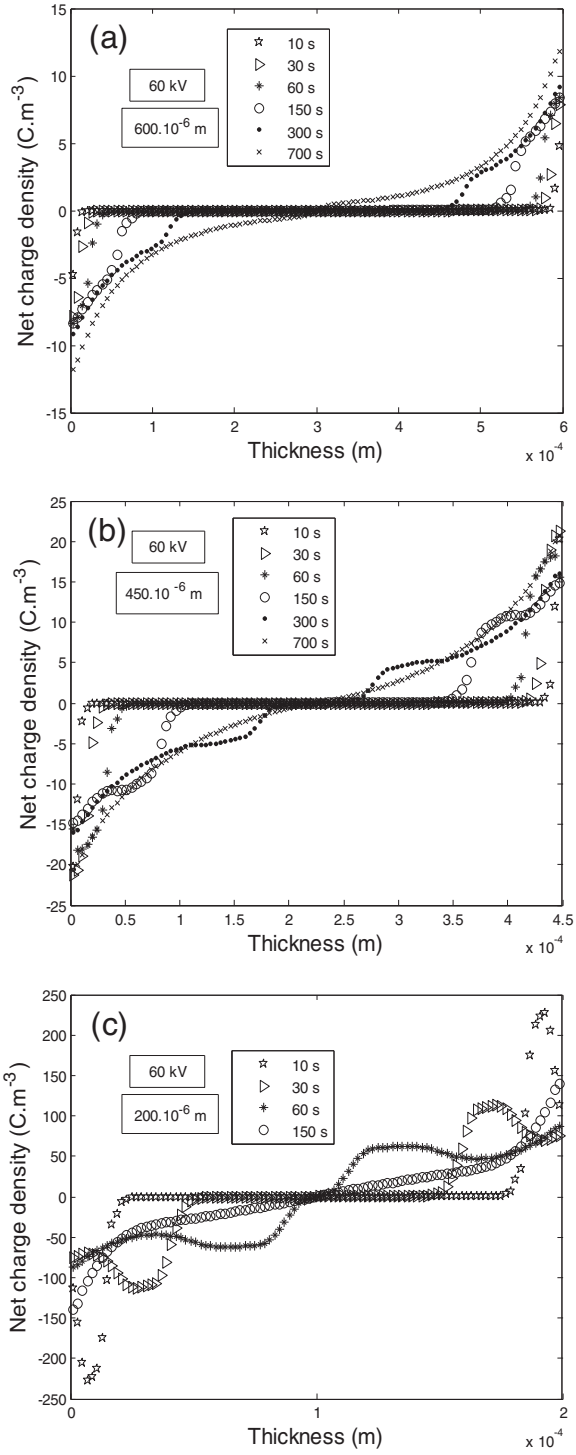

Figure 5 Net charge density under 60 kV. Thicknesses at (**a**) 600 × 10^{-6}, (**b**) 450 × 10^{-6}, and (**c**) 200 × 10^{-6} m.

For applied voltages higher than the threshold value (20 kV), we observed that the charge dynamic is inverted (Figure 4a,b). In this case, the charge dynamic is so dominated by mobile charges.

Effect of polyethylene thickness

Now, we study the effect of the sample thickness for a given dc applied voltage. In fact, from Equation 12, it is pointed out that the decrease of the sample thickness (D) has an effect similar to the increase of the applied voltage. Figure 5a,b,c shows the net charge density under 60-kV dc applied voltage in LDPE samples of 600-, 450-, and 200-μm thicknesses, respectively. These thickness values correspond to 10^8, 1.33 × 10^8, and × 10^8 V m^{-1}, respectively. These figures lead to the existence of a threshold value of thickness from which the charge packets appear and the charge dynamic changes. For example, from Figure 5a, we note the absence of the charge packets which begin to appear at a thickness of 450 μm (Figure 5b) and

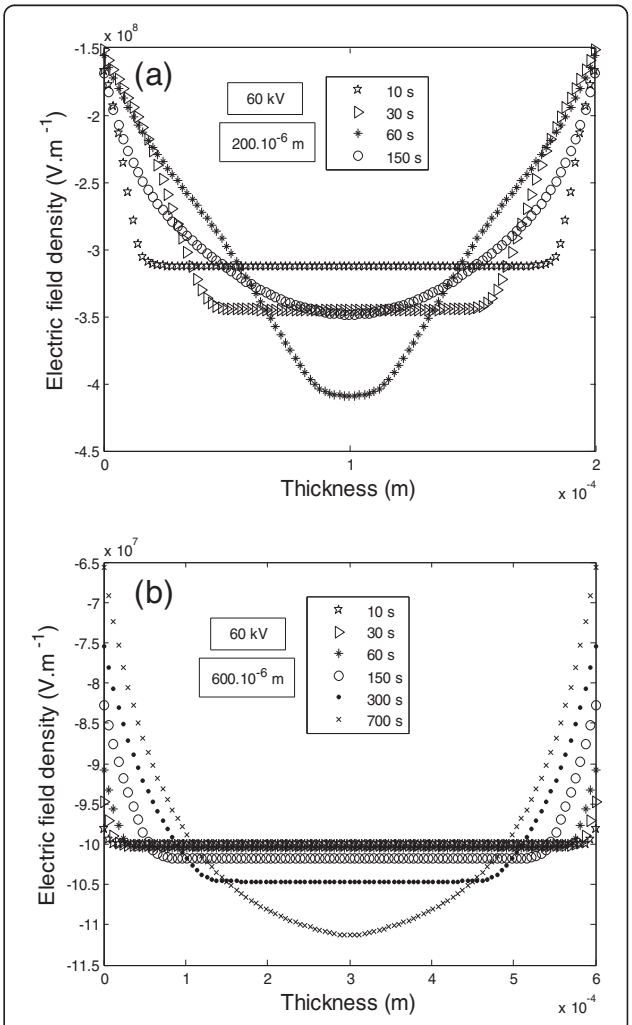

Figure 6 Electric field distribution under 60 kV. Thicknesses at (**a**) 200 × 10^{-6} and (**b**) 600 × 10^{-6} m.

clearly formed and appeared at 200 μm (Figure 5c). Thus, 450 μm is considered as the threshold thickness.

As interpreted, the apparition of charge packets is due to the reintensification of the interfacial electric field. In fact, we note in Figure 6a the reintensification of the interfacial electric field at 200 μm; however, it decreased continuously until 600 μm (Figure 6b).

In order to study the effect of the sample thickness on the charge dynamic, we represent in Figures 7a,b and 8a, b the densities of mobile and trapped electrons under 60-kV dc applied voltage at 600 and 200 μm, respectively. At 600 μm, it is clear to see that the trapped electron density is much higher than the mobile electron density; for example, at 700 s, the ratio between the trapped density (Figure 7a) and the mobile density (Figure 7b) near the electrodes is greater than 4. Hence, the conclusion is that the charge dynamic for thicknesses greater than 450 μm is governed by trapped charges.

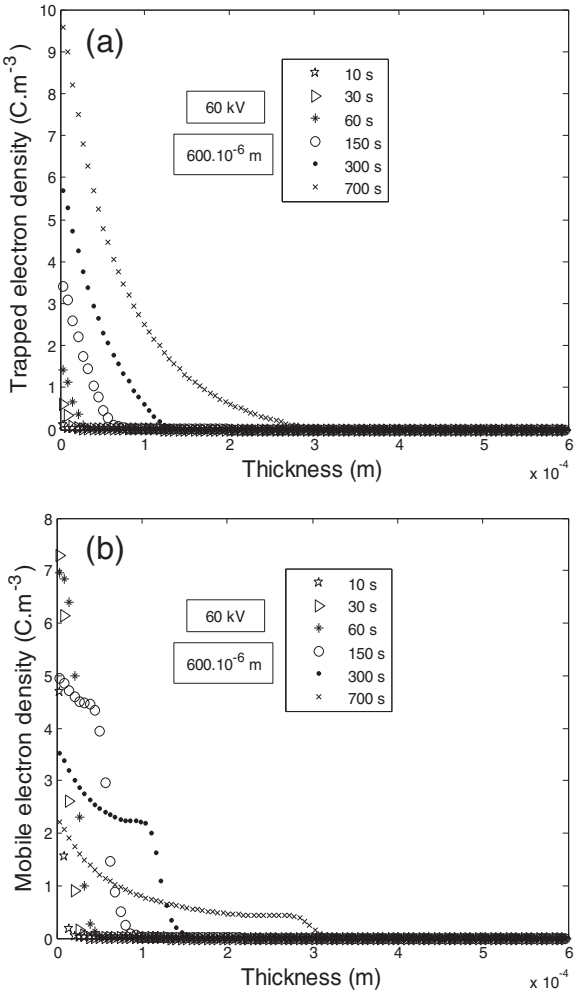

Figure 7 Mobile and trapped electron densities in a thickness of 600 × 10^{-6} m under 60 kV. (**a**) Trapped electron density and (**b**) mobile electron density.

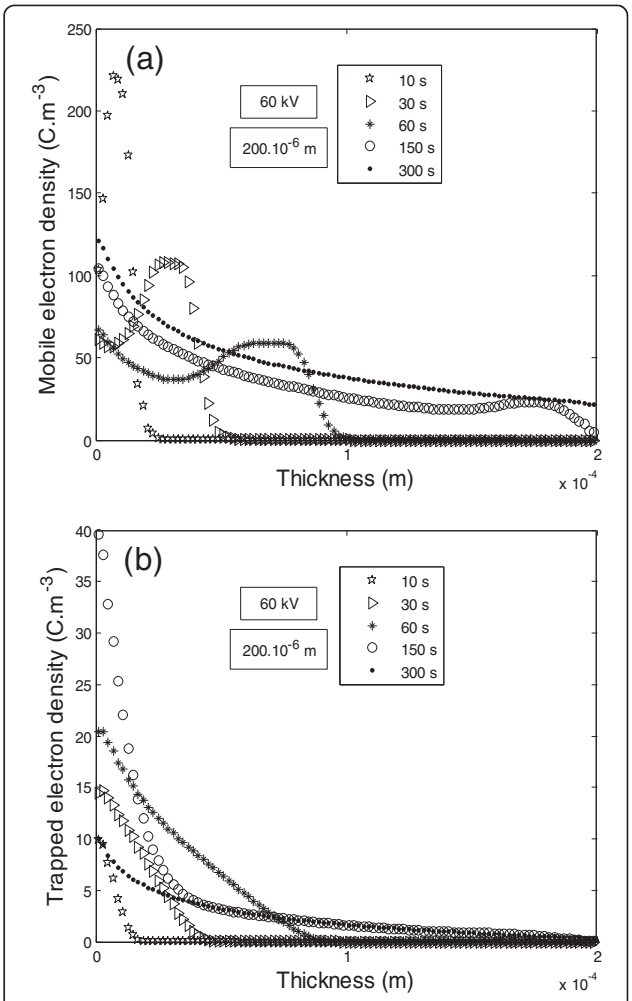

Figure 8 Mobile and trapped electron densities in a thickness of 200 × 10^{-6} m under 60 kV. (**a**) Mobile electron density and (**b**) trapped electron density.

This aspect inverts for thicknesses less than 450 μm where the mobile electron density (Figure 8a) becomes much more important than that of the trapped electrons (Figure 8b), and the ratio between mobile and trapped densities near to the electrodes is greater than 10. Therefore, the charge dynamic for thicknesses less than 450 μm is dominated by mobile charges.

Conclusions

In this paper, we studied the space charge dynamic in an additive-free low-density polyethylene and the conditions of space charge packet apparition. Model results proved the existence of a threshold electric field of 1.33 × 10^8 V m^{-1} (20-kV dc applied voltage) from which the charge packets appear and the charge dynamic becomes governed by mobile charges. In addition, we investigated in this study the effect of polyethylene thickness on the apparition of space charge packets. It should be noticed that the

obtained threshold electric field corresponds to the fixed thickness of 150 μm; in the same way, the obtained threshold thickness corresponds to the fixed applied electric field of 4×10^8 V m^{-1} (60-kV dc applied voltage). Therefore, the applied electric field and the sample thickness are highly dependent from each other, and consequently, there is a threshold electric field for each thickness and a threshold thickness for each electric field. Thus, we concluded that this study gives useful information about the adequate insulator thickness that should be chosen when the applied electric field is fixed.

Competing interests
The authors declare that they have no competing interests.

Authors' contributions
IB and EB developed the theoretical part and the modeling program. AG and AK performed the calculation. All authors read and approved the final manuscript.

Received: 25 October 2012 Accepted: 17 May 2013
Published: 11 June 2013

References

1. Deschamp, L, Caillot, C, Paris, M, Perret, J: Revue Générale de l'Electricite. **5**, 343–360 (1983)
2. Bougharriou, A, Hachicha, O, Kallel, A, Blaise, G: Effect of current density on electron beam induced charging in MgO. Nucl. Inst. and Methods in Phys. Research. B **240**, 697–703 (2005)
3. Dissado, LA, Fothergill, JC: Electrical Degradation and Breakdown in Polymers. Peter Peregrinas Ltd, London (1992)
4. Teyssedre, G, Laurent, C: Charge transport modeling in insulating polymers: from molecular to macroscopic scale. IEEE Trans Dielectr Electr Insul **12**, 857–875 (2005)
5. Alison, JM, Hill, RJ: Phys. D: A model for bipolar charge transport, trapping and recombination in degassed crosslinked polyethene. Appl Phys **27**, 1291–1299 (1994)
6. Le Roy, S, Segur, P, Teyssedre, G, Laurent, C: Description of charge transport in polyethylene using a fluid model with a constant mobility: model prediction. J. Phys. D: Appl. Phys. **37**, 298–305 (2004)
7. Kaneko, K, Suzuoki, Y, Mizutani, T: Computer simulation on formation of space charge packets in XLPE films. IEEE Trans Dielectr Electr Insul **6**, 152–158 (1999)
8. Fukuma, M, Nago, M, Kosaki, M: Computer analysis on transient space charge distribution in polymer. Pro 4th Int Conf. on Properties and Applications of Dielectric Materials **1**, 24–27 (1994)
9. Boufayed, F, Teyssèdre, G, Laurent, C, Le Roy, S, Dissado, LA, Ségur, P, Montanari, GC: Models of bipolar charge transport in polyethylene. J Appl Phys **100**, 104105 (2006)
10. Belgaroui, E, Boukhris, I, Kallel, A, Teyssedre, G, Laurent, C: A new numerical model applied to bipolar charge transport, trapping and recombination under low and high dc voltages. J. Phys. D: Appl. Phys. **40**, 6760–6767 (2007)
11. Belgaroui, E, Boukhris, I, Kallel, A: Transient and steady-state currents in polyethylene film under low and high dc voltages. Eur Phys J Appl Phys **48**, 20404 (2009)
12. Chen, G, Han Loi, S: Mater. Res. Soc. Symp **889**, W08–06-1 (2006)
13. Meunier, M, Quirke, N: Molecular modeling of electron trapping in polymer insulators. J Chem Phys **113**, 369–376 (2000)
14. Meunier, M, Quirke, N: Molecular modeling of electron traps in polymer insulators: chemical defects and impurities. J Chem Phys **115**, 2876–2881 (2001)

doi:10.1186/2251-7235-7-29
Cite this article as: Gargouri *et al.*: **Packet charge dynamic in thin polyethylene under high dc voltage.** *Journal of Theoretical and Applied Physics* 2013 **7**:29.